

Upper Bound of Accuracy for Self-Calibration of an 3D Ultrasound Tomography System without Ground Truth

Wei Yap Tan¹, Till Steiner², and Nicole V. Rüter¹

¹*Karlsruhe Institute of Technology, Germany*

Email: wei.tan@kit.edu

²*Pepperl+Fuchs GmbH, Germany*

Abstract

A self-calibration method was presented for a 3D Ultrasound Tomography System (USCT) in IEEE Ultrasonics Symposium (IUS) 2015 [1]. The method sequentially calibrates a complex USCT system with 2041 transducers based on time-of-flight (TOF) measurements. A direct evaluation of the calibration result was not possible due to unknown ground truth. In this work we present a method to estimate the upper boundary for the calibration accuracy. Evaluation with experiment data shows an estimated upper boundary of the mean error of 0.11 mm, which is smaller than the required accuracy of $\lambda/4 = 0.15$ mm for high quality image reconstruction [2].

Keywords: self-calibration, calibration accuracy, upper boundary

1 Introduction

The current 3D USCT system at KIT has a semi-ellipsoidal arrangement of 2041 ultrasound transducers, which are grouped into 157 transducer arrays (TAS) with four emitters and nine receivers each as shown in Figure 1. These transducers have a center frequency of 2.5 MHz with 50 % bandwidth and an opening angle of approximately 30° at -6 dB.

The semi-ellipsoidal aperture has a diameter of 26 cm and a depth of 18 cm. Additional virtual positions of the ultrasound transducers can be achieved by applying translational and rotational movements to the aperture.

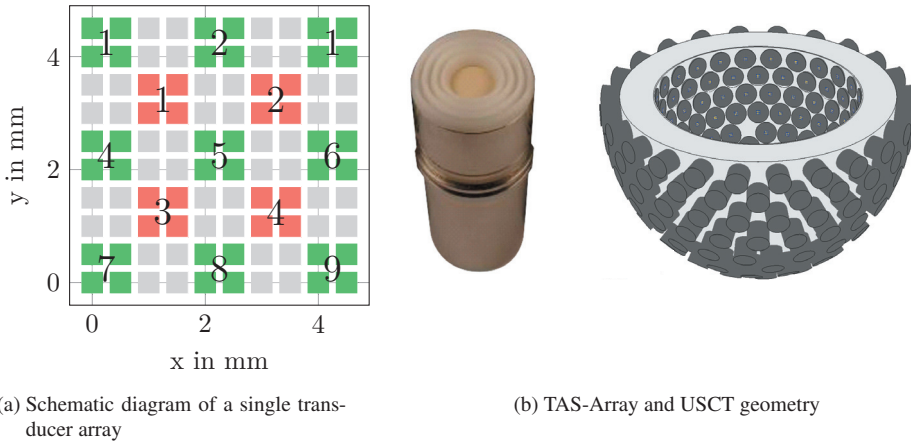


Figure 1: The figures shows the current setup of the USCT.

It is a challenging task to manually calibrate the USCT due to the large amount of transducers and data acquisition channels. Possible error sources in USCT are position errors, temperature errors, delay errors and malfunctioning transducers. For high quality reconstruction of objects in the ROI of USCT, a TOF error less than one fourth of the wavelength ($\lambda/4$) is required [2] for the reconstruction of reflectivity image with the synthetic aperture focusing technique (SAFT) [3].

A self-calibration method based on time-of-flights (TOF) between the emitters and receivers was introduced in [1]. The self-calibration method is capable of separating each potential error sources and sequentially calibrate them by solving nonlinear equation systems with the Newton's method.

The proposed method was evaluated with simulated and experiment data. In the simulations, the capability of the method in quantifying and compensating multiple error sources was shown. However, a direct evaluation of the calibration accuracy with the experiment data was not possible due to the unknown ground truth. In this work we present a method to estimate the upper boundary for the calibration accuracy.

2 Methods

The goal of this work is to provide an estimation on the calibration accuracy for USCT under the absence of the ground truth. As the self-calibration method calibrates the USCT based on TOF between emitters and receivers with nonlinear equation systems, the calibration accuracy can be given by investigating the error propagation in these equation systems. The errors considered are errors in the detected TOF as input data of the equation systems.

2.1 Error Propagation in Equation Systems

In numerical mathematics, the condition number κ is used to describe the error propagation in equation systems [4]. The condition number shows how a small change in the input data is reflected in the function values for an equation system. In terms of error propagation, the condition number quantifies the sensitivity of the equation system against errors in the input data.

The determination of the condition number for a nonlinear equation system is performed by applying numerical methods. According to [4], the condition number for a nonlinear equation system is calculated by

$$\kappa = \frac{\|J(\mathbf{x})\|}{\|f(\mathbf{x})\| \|\mathbf{x}\|}. \quad (1)$$

For each calibration step, the maximum condition number κ_{max} of the equation systems is estimated by repeated evaluations of the Eq. (1) at a point \mathbf{x} with small changes $\delta\mathbf{x}$. The points \mathbf{x} are for instance the transducer positions and the expected delays in USCT.

In general, an equation system with a condition number $\kappa \geq 1$ is characterized as well conditioned. If κ is much greater than 1, the equation system is considered poorly conditioned. Whereas, for $\kappa = \infty$ the equation system has no solution [4].

The relative error of the solution $\frac{\|\Delta\mathbf{x}\|}{\|\mathbf{x}\|}$ of an equation system can be calculated with the maximum condition number κ_{max} and the relative input error $\frac{\|\Delta\mathbf{b}\|}{\|\mathbf{b}\|}$ as in Eq. (2).

$$\frac{\|\Delta\mathbf{x}\|}{\|\mathbf{x}\|} \leq \kappa_{max} \cdot \frac{\|\Delta\mathbf{b}\|}{\|\mathbf{b}\|} \quad (2)$$

The input error $\|\Delta\mathbf{b}\|$ can be determined from the experimental data of USCT under controlled environment. For example, we conducted in this work a series of consecutive empty measurements of USCT without objects in the aperture. It was assumed that the transducer positions were fixed and the temperature distribution in the water was known. The input error $\|\Delta\mathbf{b}\|$ is then the maximum deviation of the detected TOF for each emitter-receiver-combination in these measurements.

Since the numerical methods used for solving nonlinear equation systems requires the inversion of the Jacobian matrix, it is important to check the Jacobian matrix for singularity in each iteration step. A Jacobian matrix contains the first-order partial derivatives of an equation system. One method for detecting the singularity is to calculate the determinant of the Jacobian matrix. A Jacobian matrix is singular when the determinant is equal to zero.

2.2 Residual of the Calibration

When solving an equation system $\mathbf{F}(\mathbf{x}) = \mathbf{b}$ with numerical methods such as the Newton's method, the result $\hat{\mathbf{x}}$ is an approximation of the actual solution \mathbf{x} . The residual \mathbf{r} is given by

$$\mathbf{r} = \mathbf{b} - \mathbf{F}(\hat{\mathbf{x}}). \quad (3)$$

The minimization of the residual is often used to systematically improve the solution in iterative methods. In addition to the maximum iteration, it can be used as a termination criterion when solving the equation systems.

In the absence of ground truth, the residual can be used to measure the accuracy of the approximated solution. The solution $\hat{\mathbf{x}}$ is considered close to the actual solution \mathbf{x} when the residual is small. In the self-calibration method, the residual of the equation systems is calculated in each calibration step using the unit meter.

2.3 Calibration Accuracy

In this work, the calibration error $\hat{\varepsilon}$ is estimated by

$$\hat{\varepsilon} = \underbrace{|\Delta\mathbf{b}| \cdot c \cdot \sum_i^N \kappa_{max,i}}_{\text{Error in equation system}} + \overbrace{\sum_i^N r_i}^{\text{Residual}}, \quad (4)$$

with N as the number of calibration steps. The variable c is the speed of sound in the medium. In Eq. (4), the calibration error consists of two terms. The first term contains the amplification of the TOF errors $|\Delta\mathbf{b}|$ through the equation systems. The second term is the residual of the equation systems. Fig. 2 shows an example of the calibration error estimation in one calibration step with an equation system consisting of two unknowns.

In Fig. 2, the upper boundary of the calibration errors due to error propagation in the equation system is plotted with the blue circle around the exact solution \mathbf{x}_0 . This upper boundary is further enlarged with the residual r of the equation system as shown by the gray dashed circle.

According to Eq. (4), the calibration error can be reduced by minimizing the TOF errors $|\Delta\mathbf{b}|$ and the condition number κ_{max} in each calibration step. The minimization of the condition number can be achieved by maximizing the ratio between the number of equations to the number of unknowns in the equation system. This reduces the contribution of each TOF error in the approximated solution. In the self-calibration method, the number of equations can be increased by including more emitter and receiver combinations.

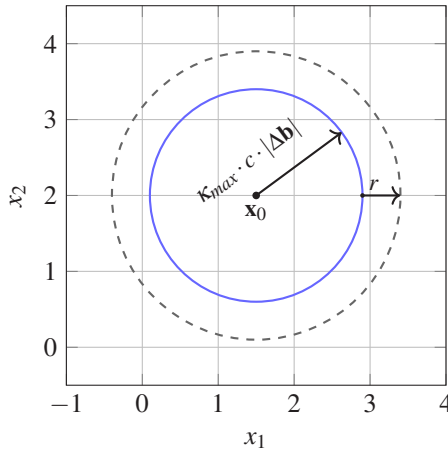


Figure 2: The figure demonstrates the estimation of calibration error for an equation system with two unknowns x_1 and x_2 with one calibration step. The exact solution of the equation system is x_0 .

On the other hand, the TOF errors can be reduced by excluding A-scans with low signal-to-noise ratio (SNR) or malfunctioning transducers and electronics. This strategy contradicts with the idea of minimizing the condition number with more emitter-receiver-combinations. As the ultrasound transducer has a limited opening angle, increasing the emitter-receiver-combinations requires using A-scans from larger transmitting and receiving angles, which have lower SNR.

From this we conclude that the minimization of calibration errors can only be achieved by compromising between minimization of the condition number and TOF errors. Hence, a careful selection of emitter-receiver-combinations for the calibration is crucial for a good calibration result.

3 Evaluation with USCT

In this section, we investigated the relationships between the amount of emitter-receiver-combinations included for the calibration, the condition number in each calibration step and the TOF error. In the self-calibration method in [1], the angle α is used to select receivers with an angle to the normal vector of each emitter smaller than this angle.

A-scans from these selected emitter-receiver-combinations are used for the calibration. Due to the semi-ellipsoidal form of the USCT aperture, TAS in the lower part will not be calibrated. Table 1 shows the calibrated TAS of USCT with different values of the angle α . For a complete calibration of all TAS in USCT, a minimum angle α of 45° is needed.

Angle α	10°	20°	30°	40°	$\geq 50^\circ$
Number of calibrated TAS	72	114	138	150	157

Table 1: Number of calibrated TAS in USCT with different values of the angle α

The condition number of each calibration step is computed for the angle $\alpha = 10^\circ \dots 60^\circ$ and shown in Fig 3. The condition number reduces with more emitter-receiver combinations used for the calibration except for the position calibration. Despite this, the overall condition number improves with larger angle α .

In order to determine the TOF error $|\Delta \mathbf{b}|$, ten consecutive empty measurements were performed with USCT. During the measurements, the positions of the ultrasound transducers were assumed to be constant and the water temperature was monitored. The TOF errors were then computed for angle α from 10° to 60° and plotted in Fig 4.

According to Fig. 4 the maximum TOF error increases rapidly from angle α larger than 20° and reaches the used detection window of $2 \mu\text{s}$ during the TOF detection with matched filter.

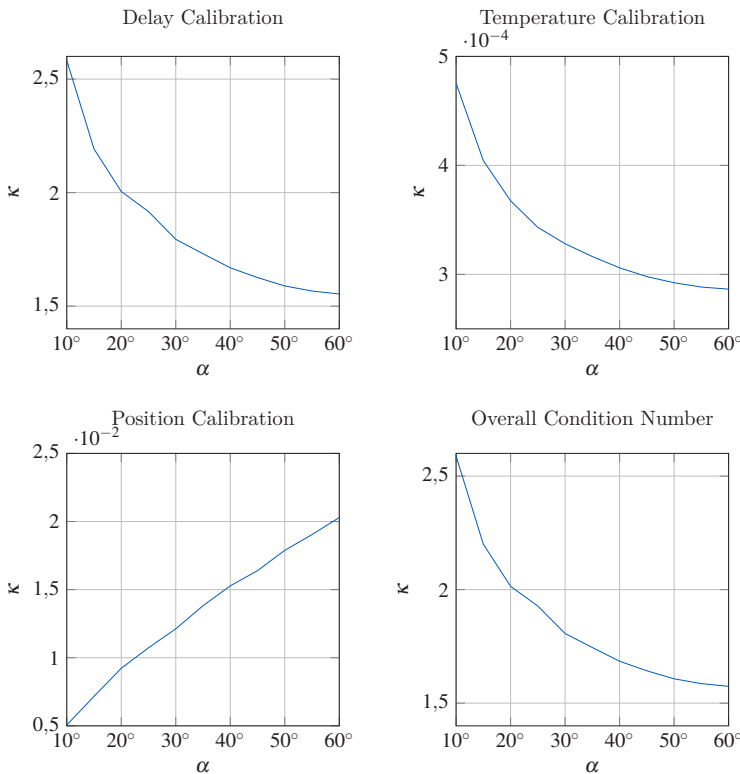


Figure 3: The figure shows the condition number κ_{max} of each calibration step according to the angle α .

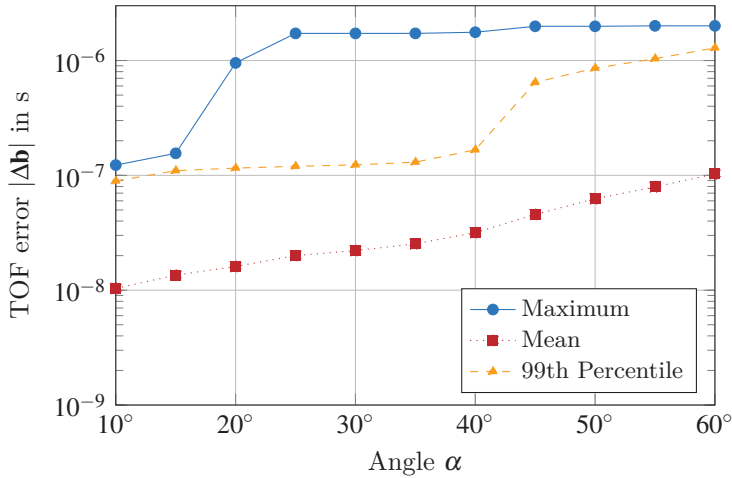


Figure 4: The figure shows the TOF errors for different angles α .

This rapid increase is caused by the fact that some A-scans with bad SNR were not sorted out in the filtering process and appear as outliers in the statistic.

The 99th percentile confirms this assumption as shown in Figure 4. For angles α smaller than 40° , the TOF error was approximately $0.1 \mu\text{s}$. Meanwhile, the plotted mean TOF error shows an increase in TOF errors with larger angle α as expected.

The investigation proved that the minimization of both the condition number and the TOF error to be a contradicting process. For the calibration of all TAS in USCT, the angle α was set at 45° . Table 2 lists the estimated calibration errors with a water temperature of 30°C during the measurements. The total residual was significantly smaller than the TOF error in the order of 1×10^{-7} . A mean calibration error of 0.11 mm was estimated for a total condition number $\kappa_{all} = 1.64$.

	$ \Delta\mathbf{b} $	$ \Delta\mathbf{b} \cdot c$	$ \Delta\mathbf{b} \cdot c \cdot \kappa_{all}$
Mean	45.68 ns	68.95 μm	0.11 mm
0,99-Perzentil	0.64 μs	0.97 mm	1.60 mm
Maximum	1.98 μs	3.00 mm	4.90 mm

Table 2: Calibration error with $\alpha = 45^\circ$

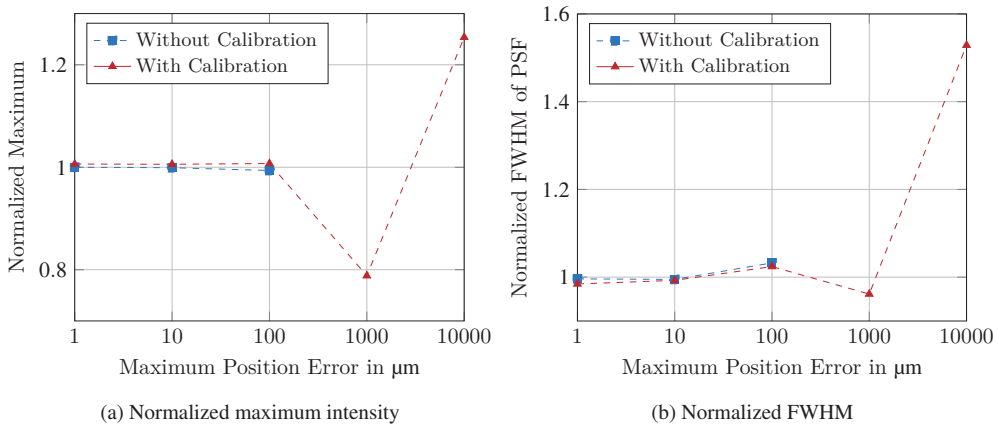


Figure 5: The figure shows the maximum intensity and FWHM of the PSF of the reconstructed point scatterer normalized to the ground truth with and without the calibration. The image quality is closest to the ground truth with both normalized values nearest to one. The reconstructions without calibration failed to produce a focused image for errors larger than 1 mm.

4 Improvements in the Image Quality

One critical aspect during the construction of the 3D USCT is the machining accuracy required for the aperture and the transducer arrays. The current version of USCT was built with an accuracy of $10\ \mu\text{m}$, which implied large technical efforts and costs. The possibility to build the USCT at a coarser accuracy and calibrate the transducer positions will hence be beneficial.

In the following investigation, the USCT was simulated with maximum position errors of individual transducer in a range between $1\ \mu\text{m}$ and 1 cm. For each maximum position error an empty measurement and a measurement with a point scatterer in the middle of the USCT aperture were simulated. The A-scan was sampled at 10 MHz. In order to achieve high accuracy in the simulated TOF of the transmission and reflection signal, fractional delay filter in the Fourier space was used [6]. Other error sources such as delays and temperature errors were not simulated.

The transmitted coded excitation is a chirp signal with a start frequency at 1.66 MHz and a stop frequency at 3.33 MHz. The TOF detection was performed with a matched filter at 10 MHz sample rate. For the image reconstruction, a SAFT reconstruction with speed of sound and attenuation correction was used [7] and the image resolution was $10\ \mu\text{m}$.

In Figure 5, the maximum intensity and the full width at half maximum (FWHM) of the point spread function (PSF) [8] of the reconstructed point scatterer was normalized to the ground truth. The image quality is closest to the ground truth with both normalized values nearest to one.

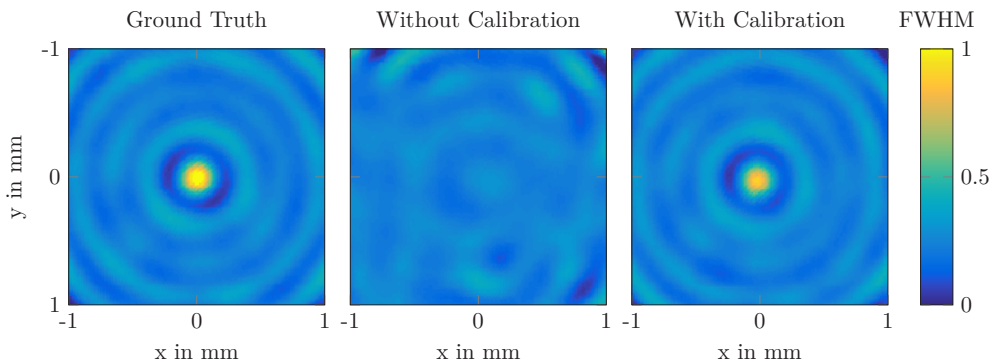


Figure 6: The figure compares the reconstructed point scatterer with and without calibration to the ground truth at maximum position error of 1 mm.

The resulting images were similar to the ground truth for reconstructions with and without calibration for maximum position errors under $100\ \mu\text{m}$, which is smaller than $\lambda/4 = 152\ \mu\text{m}$ of the center frequency at 2.5 MHz.

For maximum position errors larger than 1 mm, the reconstruction without calibration failed to produce a focused image of the point scatterer as shown in Figure 6. The reconstruction with calibrated USCT at maximum position error of 10 mm has a higher maximum but a larger FWHM than the ground truth.

5 Conclusion

In this work, we proposed a method for estimating the upper boundary of the calibration error of USCT based on the investigation of the error propagation in equation systems. An upper boundary of the mean calibration error of 0.11 mm was estimated with the experiment data of ten consecutive measurements under controlled environment, which is smaller than one fourth of the wavelength used as required for high quality image with USCT [2].

The evaluation also showed that the minimization of the calibration error is a tradeoff between minimizing the condition number κ and the TOF error. The estimation method enables finding the optimal selection of emitter-receiver combinations to obtain the smallest upper boundary of the calibration error.

In Section 4, the simulations of a point scatterer with different maximum errors in the transducer positions demonstrates the improvements in the image quality with the self-calibration. It was also showed that for the current USCT system, a machining accuracy of $100\ \mu\text{m}$ would be sufficient for usable image quality when neglecting other error sources such as delays, jitters in the electronics and temperature errors. The investigation also showed that the self-calibration

was able to calibrate position errors up to 1 mm and reconstructs focused image comparable to the ground truth as shown in Figure 6.

References

- [1] Tan, W. Y., Steiner, T., and Rüter, N. V. Newton's method based self calibration for a 3D ultrasound tomography system. In *Ultrasonics Symposium (IUS), 2015 IEEE International* (2015).
- [2] Schwarzenberg, G. F. *Untersuchung der Abbildungseigenschaften eines 3D-Ultraschall-Computertomographen zur Berechnung der 3D-Abbildungsfunktion und Herleitung einer optimierten Sensorgeometrie*. PhD thesis, Universität Fridericiana zu Karlsruhe (TH), 2008.
- [3] Stepinski, T. An implementation of synthetic aperture focusing technique in frequency domain. *IEEE Transactions on Ultrasonics, Ferroelectrics, and Frequency Control* 54, 7 (2007), 1399–1408.
- [4] Trefethen, L., and Bau, D. *Numerical Linear Algebra*. Society for Industrial and Applied Mathematics (SIAM, 3600 Market Street, Floor 6, Philadelphia, PA 19104), 1997.
- [5] Neuß, N. *Einführung in die Numerische Mathematik für Studierende der Fachrichtungen Informatik und Ingenieurwesen*, 2011.
- [6] Laakso, T., Välimäki, V., Karjalainen, M., and Laine, U. Splitting the unit delay - tools for fractional delay filter design. *IEEE SIGNAL PROCESSING MAGAZINE* (1996), 30–60.
- [7] Rüter, N. V., Kretzek, E., Zapf, M., Hopp, T., and Gemmeke, H. *Time of flight interpolated synthetic aperture focusing technique*, 2017.
- [8] Suetens, P. *Fundamentals of Medical Imaging*. Cambridge medicine. Cambridge University Press, 2009.